ELSEVIER

Biophysical Chemistry 74 (1998) 99–106

Biophysical Chemistry

Determination of protein association constants by electrophoresis

Reginald Matejec*, Hansjürgen Schönert

Institut für Physikalische Chemie, Rheinisch — Westfälische Technische Hochschule Aachen, D-52062 Aachen, Germany

Received 23 February 1998; accepted 30 April 1998

Abstract

An electrophoresis cell with scanning UV-absorption optics is presented. It allows the measurement of moving reaction boundaries of dilute protein solutions with a high-resolution. The protein profiles in the boundaries can be extrapolated to infinite time after an appropriate transformation of space and time coordinates and then evaluated with respect to association constants. This is demonstrated for the dimer–tetramer equilibrium of haemoglobin.

Keywords: Association equilibria; Haemoglobin; Electrophoresis

1. Introduction

The determination of dissociation constants in solutions by non-equilibrium transport experiments has its origin from Ostwald's dilution law: the electrical conductivity of a series of homogeneous solutions of varying concentrations of a weak acid gives the desired answer. This method is not feasible for dissociating/associating proteins because of the swamping conductivity of the buffer. Instead, one uses the concentration profiles of moving boundaries which show deviations from the ideal gaussian behaviour, leading even to bimodal peaks if more than two subunits M associate to a polymer P: $nM \leftrightarrow P$. The non-linear differential equations describing these moving boundaries have been solved either by numerical methods [1–5] or analytically for the asymptotic case of negligible diffusion [1,2,6,7].

This moving boundary method rests on two assumptions: (1) the concentration changes caused by the dissociation/association reactions must be fast compared to the concentration changes induced by the transport, i.e. local equilibria obtain at every moment in all volume elements; (2) the mobilities of the species, here M and P, should be sufficiently different. These conditions are fulfilled for a wide class of reactions in protein solutions.

* Corresponding author.

0301-4622/98/$19.00
PII S0301-4622(98)00169-0

Of all the possible reaction boundaries the one with a dimerizing protein is the most difficult to analyze because the deviation from the gaussian behaviour is the least pronounced one. This means that only the change of the boundary during an electrophoretic run may give us enough information to extract the equilibrium constant. With this aim in view we have built an appropriate electrophoresis cell with scanning UV-absorption optics and we have tried to find conditions for the measurement and evaluation of the moving boundary of the dimer–tetramer equilibrium of human haemoglobin [8] as an example.

2. Theory

We present the theory [1–7] as far as it is necessary for the understanding of the concept and the evaluation of the experiment.

If one takes the establishment of the local equilibrium for granted, as we do, the transport of the solute constituent is described by

$$\frac{\partial c}{\partial t} = \frac{\partial}{\partial x}\left[D\frac{\partial c}{\partial x}\right] - \frac{\partial}{\partial x}(c\bar{v}) \tag{1}$$

where c is the concentration of the constituent (in mass per volume), D the (species averaged) diffusion coefficient and $\bar{v}$ the migration velocity. As usual, t denotes the time and x the space coordinate.

For the dimer–tetramer equilibrium

$$2D = T$$

there are

$$c = c_D + c_T \tag{2}$$

$$\bar{v} = (c_D v_D + c_T v_T)/c \tag{3}$$

$$K = c_T/(c_D)^2 \tag{4}$$

Here, the subscripts D and T refer to the species dimer and tetramer. In the mass action law Eq. (4) the activity coefficients can be thought of as either being incorporated into the equilibrium constant K or given by the assumption of Adams and Fujita [9].

The different species velocities v_D and v_T try to spread an initial concentration step of the solute proportional to time: $(v_T - v_D)\cdot t$, whereas the diffusional spreading is proportional to the square root of time: $2\sqrt{Dt}$. The ratio

$$S = (v_T - v_D)t_{\max}/2\sqrt{Dt_{\max}} \tag{5}$$

where $t_{\max}$ denotes the time of the last observation may serve as a measure of the result of these two spreading mechanism. This will be used later.

The foregoing considerations form the basis for the analytical asymptotic solution of Gilbert [6,7] and also for the measurement procedure and evaluation given here. They are described by the transformation

$$z = x/t, \quad y = 1/t \tag{6}$$

which transforms Eq. (1) to

$$z\frac{\partial c}{\partial z} + y\frac{\partial c}{\partial y} = -y\frac{\partial}{\partial z}D\frac{\partial c}{\partial z} + \frac{\partial}{\partial z}(c\bar{v}).$$

For infinite time, $y \to 0$, this reduces to

$$z\frac{\partial c^{\infty}}{\partial z} = \frac{\partial}{\partial z}(c^{\infty}\bar{v}) \tag{7}$$

Here, the diffusional spreading is eliminated. The superscript ∞ represents the extrapolation to infinite time.

The solution of this equation is

$$c^{\infty}(z) = \frac{1}{4K}\left[\frac{(v_D - v_T)^2}{(z - v_T)^2} - 1\right], 0 \le c \le c_{\max} \tag{8}$$

if for $t = 0$ one starts with a concentration step from $c = 0$ to $c = c_{\max}$. This asymptotic profile is determined by three parameters: v_T, v_D and K. Only two of these are independent because there is a measurable relationship between them: the first reduced moment m_1/m_0 of the moving boundary connects the parameters, as will be shown below.

The moments are defined by

$$m_1 = \int_{-\infty}^{+\infty} x \frac{\partial c}{\partial x} \mathrm{d}x, \tag{9a}$$

or

$$\frac{\partial m_1}{\partial t} = \int_{-\infty}^{+\infty} x \frac{\partial}{\partial x} \frac{\partial}{\partial t} \mathrm{d}x$$

and

$$m_0 = \int_{-\infty}^{+\infty} \frac{\partial c}{\partial x} \mathrm{d}x \tag{9b}$$

The integration is from the homogeneous part of the solution on one side of the boundary to the homogeneous part on the other side of the boundary; the boundary conditions are thus

$$\begin{aligned} c &= 0, && \text{for} && x \to -\infty \\ c &= c_{\max}, && \text{for} && x \to +\infty \\ \frac{\partial c}{\partial x} &= 0, && \text{for} && x \to \pm\infty \end{aligned} \tag{10}$$

Hence, these moments can be evaluated if the concentration profile $c(x,t)$ is known.

Introducing the transport Eq. (1) into these definitions one has

$$\frac{m_1}{m_0} = \bar{v}(c = c_{\max})t + x_0 \tag{11}$$

where the boundary starts at x_0. Reference to Eq. (3) and Eq. (4) shows that this reduced moment depends on the three parameters.

We can now outline the program: in a Tiselius-cell, a step boundary is established at $t = 0$ between a protein–buffer solution and the buffer solution, and at the same time a constant electrical current is applied. The moving boundary is then monitored by scanning absorption optics for several times (approx. 40 profiles in 16 h). These profiles $c(x,t)$ are evaluated to give $\bar{v}(c = c_{\max})$ according to Eq. (11) and they are transformed (see Eq. (6)) to $c(z,y)$. For constant values of $z = \text{const.}$ they are extrapolated to $y \to 0$. This procedure does away with the diffusional spreading and leads to the Gilbert profile Eq. (8). As there is no analytical solution of the differential Eq. (1) to help in the extrapolation procedure we have used a numerical integration method [3–5] to this purpose.

In order to check for the absence of disturbing effects: convection, incomplete establishment of the step boundary at the start and extrapolation errors, one can use the fact that the migration velocities v_D, v_T and $\bar{v}$ are proportional to a mobility factor u_D, u_T and $\bar{u}$ and the electrical current density I, i.e. measurements at different current densities should lead to the same extrapolated curve if mobilities instead of velocities are used. This is expected to be true between a lower bound below which S and hence the migrational spreading is too small and an upper bound where thermal convection sets in.

3. Methods and materials

In the experimental setup (Fig. 1) the electrophoresis cell sits on a fixed block. Its temperature is kept to (298 ± 0.02) K by a copper thermostat which encloses the cell completely except for the entrance and exit of the light of the optical system. This optical system is mounted on a vertically movable table. It can be adjusted by *XY*-tables and a micrometer calliper MC1. The weight of the table is compensated by a counter-weight (not shown) so that it can be easily moved for the scanning procedure. The table is held in place by four roller bearings. The motor, controlled by an optical incremental meter OIM, moves the table via the micrometer calliper MC2.

At the start of the scanning process and after approx. 5 mm of upward movement a light signal LS determines the zero point of the x-coordinate. From then on, 800 pixels of a width of $\Delta x = 50$ μm are recorded in $\Delta t = 140$ s. These conditions, together with the layout of the optical system, ensure that the absorption is recorded without distortion and with sufficient precision.

Details of the optical system can be seen in Fig. 2. The light ($\lambda = 280$ nm) enters through a quartz-glass fibre. The other parts are self-explanatory. The output of the photomultiplier is preamplified, converted with a 12-bit A/D-converter and stored by a computer for further treatment.

The standard Tiselius cell is shown in Fig. 3.

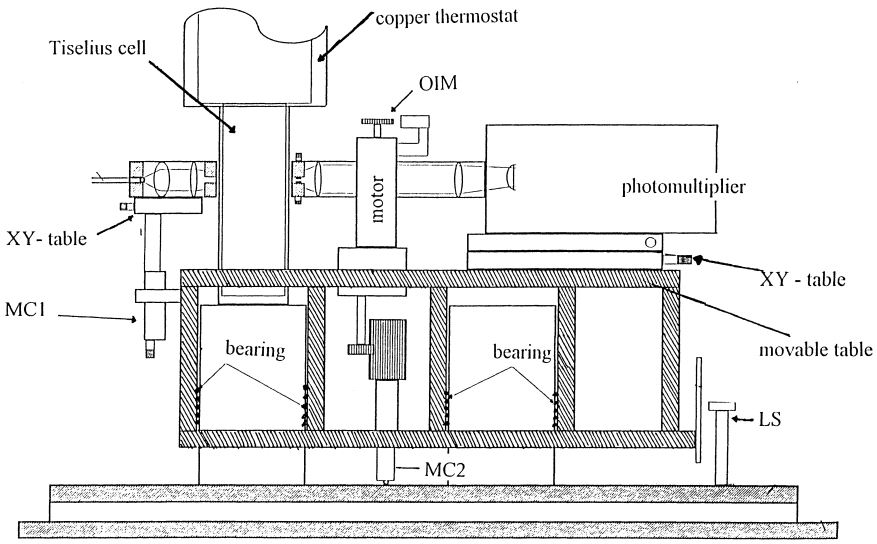

Fig. 1. The experimental setup of the electrophoresis cell with a scanning UV-absorption optics. Explanation in the text.

The lower part in which the movement of the boundary takes place is made from quartz (Hellma, Mülheim, Germany). This allows the use of the UV-light. The electrical current from a constant current source enters and leaves the solution via silver/silver chloride electrodes in aqueous KCl. One side of the cell is closed thus avoiding apparent movements of the boundary due to changing densities in the two arms of the cell.

The boundary between the buffer solution and the protein solution is sharpened by a capillary technique [10]. The syphoning capillary is withdrawn after the start of the experiment. The boundary is stabilized by 0.03 M sugar in the lower protein solution.

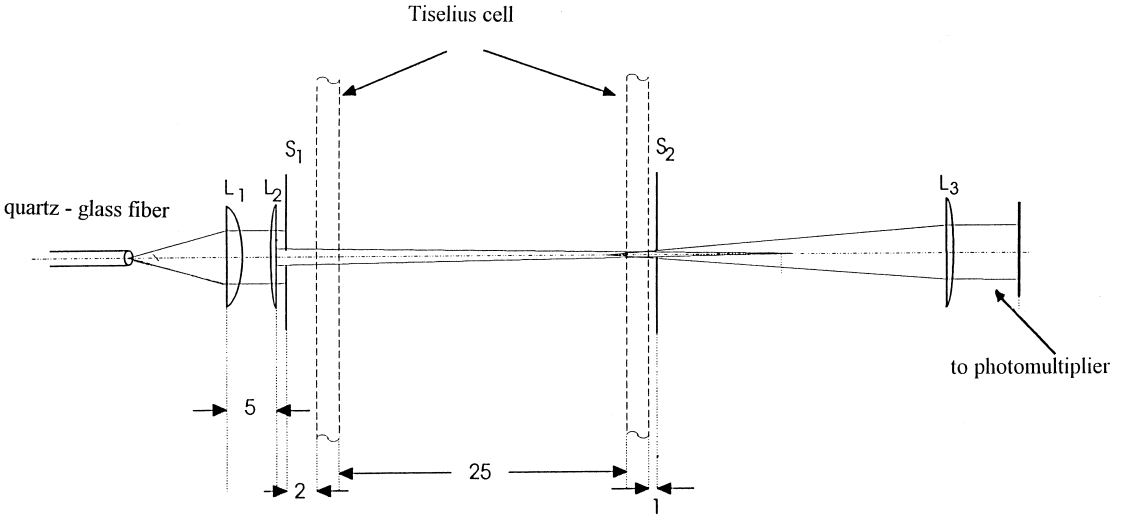

Fig. 2. The optical system. All data are given in millimetres. L_1 ($f = 13$ mm) and $L_2 = L_3$ ($f = 50$ mm) are quartz lenses; slit S_1 (width = 1 mm) and slit S_2 (width = 0.2–0.3 mm) determine the dimensions of the ray.

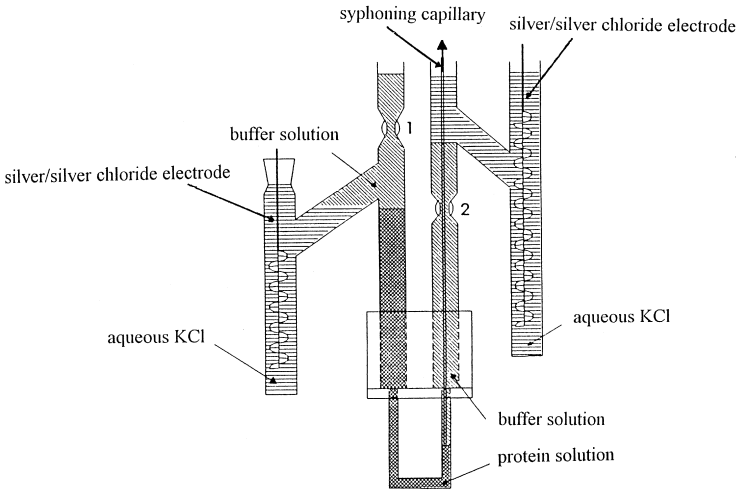

Fig. 3. The Tiselius cell.

Haemolysate of normal human blood in 0.05 M Tris, 1 mM EDTA and pH = 7.60 was concentrated with an Amicon stirred ultrafiltration cell using Amicon PM 10 membranes. The major fraction of HbA was prepared with two DEAE-Sepadex A-50 columns at 4°C according to the method of Williams and Tsay [11]. The haemoglobin concentration was determined after conversion to cyanomethaemoglobin at $\lambda = 540$ nm with $\varepsilon = 4.40 \times 10^4$ M^{-1} cm^{-1}. The content of methaemoglobin, measured spectrophotometrically with the data of Benesch et al. [12] was below 4%. At the end of an experiment it had increased approximately twofold. The haemoglobin was used in 0.1 M Tris, 1 mM EDTA, 0.2 M NaCl at pH = 7.40. The chemicals were of analytical grade. The water was bidestilled.

4. Results and discussion

We present the results of four representative experiments, Table 1. The concentration of these solutions were chosen in such a way that sufficient proportions of both dimer and tetramer species are present. This was done with known values of the equilibrium constant K [8,13]. The electrical current density varies by a factor of six. In this way one can study the influence of the migrational spreading relative to the diffusional spreading.

During each run approx. 40 profiles were taken

Table 1
The data for four experiments with haemoglobin, in 0.1 M Tris, 0.2 M NaCl, 1 mM EDTA, pH = 7.40, $T = 298$ K

No.	c/g dm^{-3}	I/mA cm^{-2}	$\bar{v}(c_{max}) \times 10^5$/cm s^{-1}	S
1	0.409	40.00	2.736	1.35
2	0.466	26.66	1.468	0.90
3	0.431	13.33	0.803	0.45
4	0.388	6.667	0.415	0.23

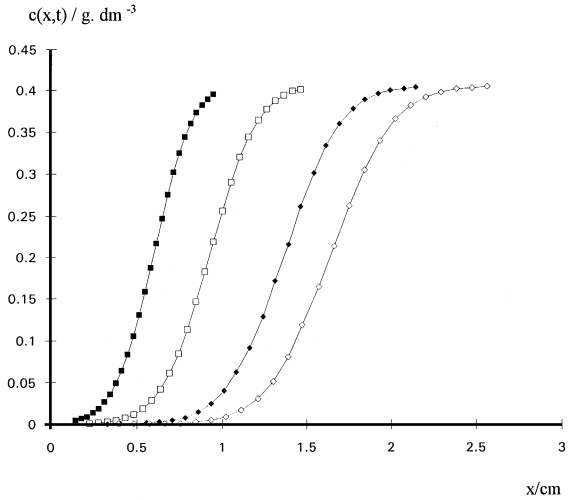

Fig. 4. Four concentration profiles for experiment 1, $t_1 =$ 22 190 s, $t_2 = 34\,460$ s, $t_3 = 50\,430$ s, $t_4 = 60\,260$s, from left to right.

in 16 h. From the first experiment we show in Fig. 4 four profiles, from $t = 22\,190$ to $t = 60\,260$ s. The starting boundary was at the origin. The last profile extends along the x-axis for approx. 2 cm. This corresponds to 400 points $c(x,t)$ only a few of which are included in Fig. 4.

These curves show no shoulder or any other obvious distortion due to the dimer–tetramer equilibrium. Only the following analysis will reveal the hidden equilibrium reaction.

All profiles were numerically treated according to Eq. (9a) and Eq. (9b) and the reduced first moment was plotted vs. time, Fig. 5. The relative standard deviation of the experimental points from a linear least-squares fit is 0.3%.

Sometimes, but rarely, one finds a change of the slope with time. The reason is a change in the temperature of the electrophoresis cell which acts like a thermometer because of the closed end of one of the electrode compartments. These experiments are not further evaluated.

From a linear least-squares fit one gets $\bar{v}(c = c_{\max})$. As it should be, it is proportional to the electrical current density, Fig. 6. The deviation from a linear fit is greater than for each of the experiments in the foregoing plot, due to slightly different concentrations $c_{\max}$ and varying contents of methaemoglobin. These deviations have no consequence for the final result because Eq. (8) is nearly immune to slight drifts.

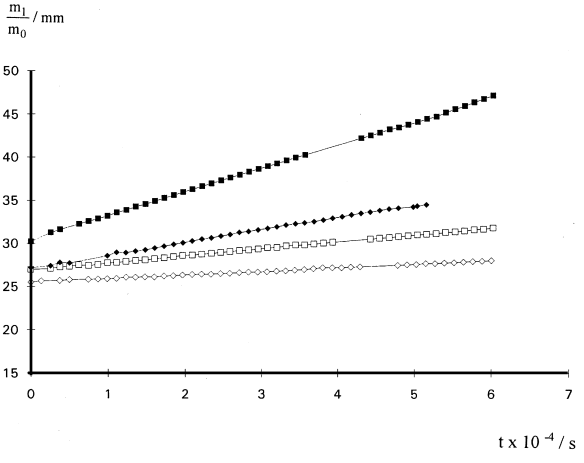

Fig. 5. The reduced first moment according to Eq. (11) for the four experiments.

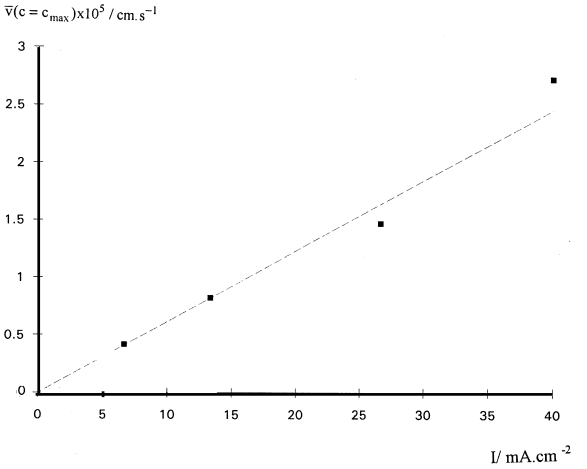

Fig. 6. The migration velocity $\bar{v}(c = c_{\max})$ as a function of the electrical current density I.

As outlined before the profiles are transformed to $c(z,y)$. A search algorithm determines for a series of transformed profiles the values $c(z_K,y)$ for several constant z_K, and these are plotted at the constant z_K vs. $y = 1/t$. Fig. 7a shows this plot for the experiment with the highest electrical current density for some values of z_K. Only guided by the eye, one can make a first extrapolation to infinite time which gives an approximate value of v_D at the point where the extrapolated curve and the x-axis cross. Together with the knowledge from the slope of the reduced first moment one can estimate K and v_T. These approximate values of the parameters serve as a starting point for a numerical integration of the differential equation where the method of Cox [3–5] has been used. The result can be used to iteratively refine the extrapolation up to some limit: a residue of errors must be tolerated because: (1) the small diffusional coupling between the stabilizing sugar and the haemoglobin is unknown; (2) the deviation of the starting boundary from a perfect step boundary is not be taken into account; and (3) the methaemoglobin content increases. Therefore and especially because the diffusion is eliminated, the exact value of the diffusion constant turns out not to be critical during the integration process: a variation of 5% is without much effect. Neverthe-

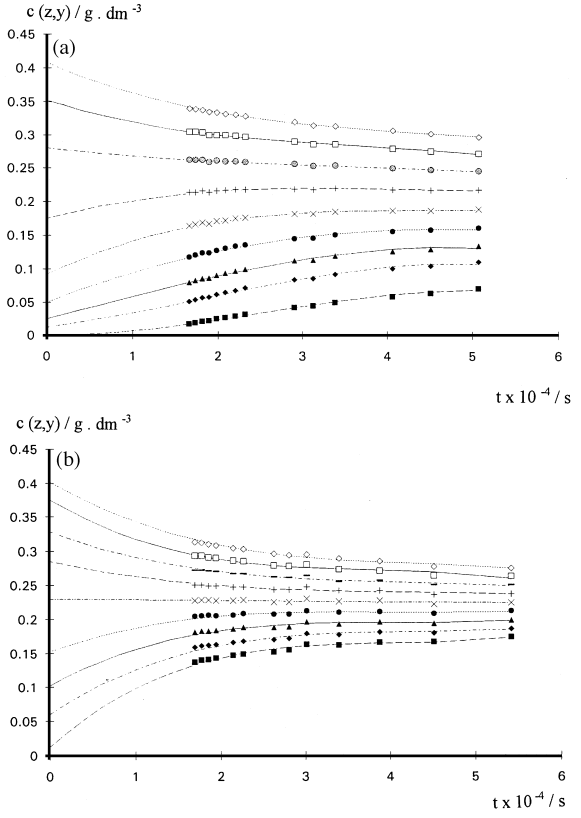

Fig. 7. (a) Experiment 1, $S = 1.35$: extrapolation for nine constants z from $z = 1.85 \times 10^{-5}$ cm s^{-1} to $z = 3.20 \times 10^{-5}$ cm s^{-1}. (b) Experiment 3, $S = 0.45$: the same from $z = 0.283 \times 10^{-5}$ cm s^{-1} to $z = 1.22 \times 10^{-5}$ cm s^{-1}.

less, the extrapolation leads to an acceptable result, Fig. 8.

In the case previously discussed, the ratio S, Eq. (5), which quantifies the two types of spreading, is $S = 1.35$. Thus, at the end of the experiment the migrational spreading slightly outweighs the diffusional spreading although the last profile in Fig. 4 apparently does not show this effect.

In the third experiment, the ratio S is smaller by a factor of three, $S \cong 0.45$, because the electrical current density is decreased by this factor. In this case the extrapolation is still possible, see Fig. 7b, but the influence of the diffusion cannot be completely removed. This is even more pronounced in the last experiment with $S \cong 0.23$ which has therefore not been further treated.

Finally, in Fig. 8 the extrapolated values are

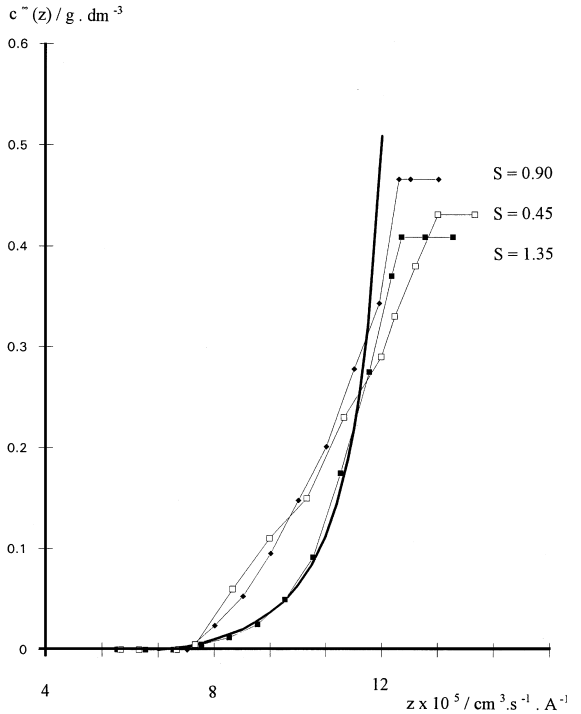

Fig. 8. The extrapolated profiles for $S = 1.35$, $S = 0.90$ and $S = 0.45$. The strong line gives the Gilbert profile Eq. (8) with $K = 10$ g^{-1} dm^3.

plotted vs. z taking mobilities instead of velocities and a corresponding use of z. Included, is a theoretical curve according to Eq. (8) with $K = 10$ g^{-1} dm^3, compared to the literature value [8,13] of $K = 14$ g^{-1} dm^3. One can see that for the $S > 1$ theory and experiment are sufficiently coincident, whereas with decreasing S the extrapolated curves depart more and more from the expected behaviour because of the insufficient elimination of the diffusional broadening.

One can conclude that this method improves the existing measurements because the scanning device with $\lambda = 280$ nm extends the concentration range well below $c = 0.1$ g dm^{-3}, and because the series of scans enables the extrapolation to infinite time and thereby the elimination of the influence of the diffusional broadening. If the electrical current density is sufficiently high even a dimerization reaction which shows the least pronounced deviation from the gaussian behaviour can be analyzed.

References

[1] J.R. Cann, Interacting Macromolecules, Academic Press, New York, 1970.
[2] L.W. Nichol, D.J. Winzor, Migration of Interacting Systems, Clarendon Press, Oxford, 1972.
[3] D.J. Cox, Arch. Biochem. Biophys. 129 (1969) 106.
[4] D.J. Cox, Arch. Biochem. Biophys. 142 (1971) 514.
[5] D.J. Cox, Arch. Biochem. Biophys. 160 (1974) 595.
[6] G.A. Gilbert, Disc. Faraday Soc. 20 (1955) 68.
[7] L.M. Gilbert, G.A. Gilbert, in: S.P. Colowick, N.O. Caplan (Eds.), Methods in Enzymology, vol. 27D, Academic Press, New York, NY, 1973.
[8] G.K. Ackers, M.L. Johnson, Biophys. Chem. 37 (1990) 265.
[9] E.T. Adams Jr., H. Fujita, in: J.W. Williams (Ed.), Ultracentrifugal Analysis in Theory and Experiment, Academic Press, New York, NY, 1963, p. 119.
[10] D.S. Kahn, A. Polson, J. Phys. Chem. 51 (1947) 8165.
[11] R.C. Williams, Jr., K.-Y. Tsay, Anal. Biochem. 54 (1973) 137.
[12] R.E. Benesch, R. Benesch, S. Yung, Anal. Biochem. 55 (1973) 245.
[13] H. Schönert, B. Stoll, Eur. J. Biochem. 176 (1988) 319.